

Attractors with the Symmetry of the n -Cube

Clifford A. Reiter

CONTENTS

Introduction

1. The Symmetry of the n -Cube

2. Equivariant Polynomial Maps

3. Experiments

Acknowledgement

References

Equivariant polynomial functions with the symmetries of the n -cube are completely determined in terms of permutations of exponents. Strategies for random searches of linear combinations of these functions are described and used to generate interesting examples of attractors. These attractors have symmetries that are an admissible subgroup of the symmetries of the square, cube and 4-cube. A central projection of the 4-cube with partial inversion is used for the illustrations of attractors in four dimensions.

INTRODUCTION

There has been much recent work on creating attractors with specified symmetry. This work has been motivated in part by the desire to understand the bifurcations that occur in physical systems such as Couette–Taylor flows, which arise in the fluid between rotating cylinders. Dozens of types of symmetry have been identified for these systems; some are described in [Stewart and Golubitsky 1992]. (Like [Weyl 1952], this reference contains an engaging introduction to the study of symmetry in the broad.)

In two dimensions, the finite fixed-point groups are the cyclic groups C_n and the dihedral groups D_n , and attractors exist with symmetries of each of these types. Striking examples can be found in [Field and Golubitsky 1990; 1992; 1995]. We will develop the theory and illustrations of attractors in n -dimensional space that have the symmetry of the n -cube.

Examples of symmetric attractors in the plane can be generated by the iteration of maps, usually polynomials, that are equivariant with respect to C_n . The polynomial invariant functions and equivariant maps for the point symmetry groups of some polytopes in various dimensions have been

studied [Patera et al. 1978; Cox et al. 1992]. The equivariant maps are often described in terms of finite generating sets. The article [Brisson et al. 1996] describes the maps equivariant under the rotational symmetries of the three-cube in two ways: in terms of finite generating sets and in terms of maps arising from permutations of exponents in the monomials. In Section 2 we generalize this to a classification of the equivariant polynomial maps that have the rotational symmetry of the n -cube.

Random linear combinations of these maps can be created in an automated manner, and analyzed under iteration. Promising examples can be used to produce images for human perception. This technique is described in Section 3, and examples of the results in dimensions up to four are given. The examples of attractors in four dimensions require careful projection in order for the symmetries to be visible; we suggest some good projections and use them in Figure 4.

Attractors in dimensions higher than two may have far richer symmetry than those in the plane because of the larger symmetry groups. For example, the symmetries of the three-cube include independent order-three and order-four turns. Figure 2 illustrates attractors exhibiting all these symmetries, and Figure 4 shows attractors having the even richer symmetries of the 4-cube.

1. THE SYMMETRY OF THE n -CUBE

The symmetry group of the n -cube is well known. We will be interested both in the full symmetry group (which includes reflections in codimension-one planes) and in the rotational, or orientation-preserving, symmetry group. One classic discussion of these symmetry groups can be found in [Coxeter 1973]: The full symmetry group of the n -cube centered at the origin with edges parallel to the axes is generated by all permutations of the axes along with the sign changes along each axis independently. This yields a group of order $2^n n!$. The orientation-preserving symmetry group is half

the size of the full group; it is generated by $n - 1$ rotations as follows.

Let R_{jk} denote a 90° rotation in the oriented jk -plane, leaving all other axes fixed. The action of R_{jk} is given by

$$R_{jk}(\dots, x_j, \dots, x_k, \dots) = (\dots, -x_k, \dots, x_j, \dots).$$

If we denote the permutation of the axes j and k by σ_{jk} and a sign change in the j -th coordinate by S_j , then $R_{jk} = \sigma_{jk} S_k = S_j \sigma_{jk}$. Moreover, $R_{jk}^2 = S_j S_k$, $R_{jk}^3 = R_{kj}$ and $R_{jk}^4 = 1$. We will number our axes beginning with 0, and distinguish axis 0 when convenient. If $j, k \neq 0$ we have $R_{jk} = R_{0k}^{-1} R_{0j} R_{0k}$. By composing rotations R_{jk} we can achieve any permutation of the axes, and at least half the choices of sign codes for that permutation, since any two coordinates can be negated via $R_{jk}^2 = S_j S_k$. Therefore the orientation-preserving group has size exactly $2^{n-1} n!$ and is generated by $R_{01}, R_{02}, \dots, R_{0n-1}$.

In particular, the orientation-preserving symmetry group of the square has 4 elements generated by a single rotation, that of the cube has 24 elements generated by two rotations, and that of the 4-cube has 192 elements generated by three rotations. In the next section we will completely describe the polynomial maps that have these symmetries.

2. EQUIVARIANT POLYNOMIAL MAPS

Suppose ρ is a symmetry of the n -cube. A map $F: \mathbb{R}^n \rightarrow \mathbb{R}^n$ is ρ -equivariant if $F(\rho(\vec{X})) = \rho(F(\vec{X}))$. The zero map, the identity map and the map

$$F(\langle x_0, x_1, \dots, x_{n-1} \rangle) = \langle x_0^5, x_1^5, \dots, x_{n-1}^5 \rangle$$

are simple examples of maps that are equivariant for all the rotations and reflections of the n -cube. In order to construct and classify more intricate examples, we will introduce the following ideas and notations. First, if $\vec{i} = \langle i_0, \dots, i_{n-1} \rangle$ is a vector of exponents and $\vec{X} = \langle x_0, \dots, x_{n-1} \rangle$ is a vector of real numbers, we define $\vec{X}^{\vec{i}} = x_0^{i_0} x_1^{i_1} \dots x_{n-1}^{i_{n-1}}$. Notice that if σ is any permutation, then $\vec{X}^{\vec{i}} = (\sigma \vec{X})^{\sigma \vec{i}}$ and hence $(\sigma \vec{X})^{\vec{i}} = \vec{X}^{\sigma^{-1} \vec{i}}$.

A vector of nonnegative integers will be said to have *tail-uniform parity* if the first element has parity different from all the others. Thus, $\langle 3, 2, 4, 0 \rangle$ and $\langle 2, 1, 3 \rangle$ have tail-uniform parity, but $\langle 1, 3, 2, 4 \rangle$ does not. If $\vec{\tau}$ has tail-uniform parity, we denote by $I = I(\vec{\tau})$ the parity of the tail: $I = 0$ if even and $I = 1$ if odd. Moreover, for a permutation σ in the symmetric group \mathfrak{S}_n , we denote by $s(\sigma)$ the parity of σ . The transformation of \mathbb{R}^n that permutes the coordinate axes according to σ is also denoted by σ ; this is the map defined by

$$\sigma(\langle x_{\sigma(0)}, x_{\sigma(1)}, \dots, x_{\sigma(n)} \rangle) = \langle (x_0, x_1, \dots, x_n) \rangle.$$

Thus if σ is the transposition σ_{12} followed by the transposition σ_{01} , we have $\sigma(\langle 3, 2, 4 \rangle) = \langle 4, 3, 2 \rangle$, since $\sigma(0) = 1$, $\sigma(1) = 2$, $\sigma(2) = 0$.

We are now ready to define the maps that are the key to classifying the polynomials equivariant with respect to the symmetry of the n -cube. Let $\vec{\tau}$ be a vector with tail-uniform parity. Then define $H_{\vec{\tau}}(\vec{X})$ as the vector whose k -th coordinate is

$$\sum_{\sigma(0)=k} (-1)^{Is(\sigma)} \vec{X}^{\sigma(\vec{\tau})},$$

for $k = 0, \dots, n-1$; here the sum is over all permutations $\sigma \in \mathfrak{S}_n$ satisfying the specified condition.

As examples with $n = 3$, consider $\vec{\tau} = \langle 3, 2, 4 \rangle$, for which

$$H_{\langle 3, 2, 4 \rangle}(\langle x, y, z \rangle) = \langle x^3 y^2 z^4 + x^3 y^4 z^2, x^4 y^3 z^2 + x^2 y^3 z^4, x^2 y^4 z^3 + x^4 y^2 z^3 \rangle$$

since $I = 0$, and $\vec{\tau} = \langle 2, 1, 3 \rangle$, for which

$$H_{\langle 2, 1, 3 \rangle}(\langle x, y, z \rangle) = \langle x^2 y^1 z^3 - x^2 y^3 z^1, x^3 y^2 z^1 - x^1 y^2 z^3, x^1 y^3 z^2 - x^3 y^1 z^2 \rangle$$

since $I = 1$. When $\vec{\tau}$ has repeated entries, the terms can combine and even collapse:

$$H_{\langle 4, 1, 1 \rangle}(\langle x, y, z \rangle) = \langle 0, 0, 0 \rangle,$$

$$H_{\langle 3, 0, 0, 0 \rangle}(\langle w, x, y, z \rangle) = \langle 6w^3, 6x^3, 6y^3, 6z^3 \rangle.$$

Theorem 2.1. *If $\vec{\tau}$ has tail-uniform parity, the map $H_{\vec{\tau}}$ is equivariant with respect to all orientation-preserving symmetries of the n -cube.*

Proof. We need only check that $H_{\vec{\tau}}(R_{0_j}(\vec{X})) = R_{0_j}(H_{\vec{\tau}}(\vec{X}))$ for $j = 1, 2, \dots, n-1$. We do this for each coordinate separately. Write $\tau = \sigma_{0_j} \circ \sigma = \sigma_{0_j}^{-1} \circ \sigma$, so that $s(\sigma) = 1 - s(\tau)$. The k -th coordinate of $H_{\vec{\tau}}(R_{0_j}(\vec{X}))$ is therefore

$$\begin{aligned} \sum_{\sigma(0)=k} (-1)^{Is(\sigma)} (\sigma_{0_j} S_j \vec{X})^{\sigma(\vec{\tau})} \\ = \sum_{\tau(0)=\sigma_{0_j}(k)} (-1)^I (-1)^{Is(\tau)} (S_j \vec{X})^{\tau(\vec{\tau})}. \end{aligned}$$

The sign change caused by S_j in $(S_j \vec{X})^{\tau(\vec{\tau})}$ is $-(-1)^I$ if $\tau(0) = j$, and $(-1)^I$ otherwise. Thus, for $k = 0$, the sum on the second line of the preceding display reduces to

$$- \sum_{\tau(0)=j} (-1)^{Is(\tau)} \vec{X}^{\tau(\vec{\tau})},$$

and this is the 0-th coordinate of $R_{0_j}(H_{\vec{\tau}}(\vec{X}))$. For $k = j$ we get

$$\sum_{\tau(0)=0} (-1)^{Is(\tau)} \vec{X}^{\tau(\vec{\tau})},$$

and for other coordinates, with $k \neq 0, j$, we have

$$\sum_{\tau(0)=k} (-1)^{Is(\tau)} \vec{X}^{\tau(\vec{\tau})}.$$

These expressions also match the corresponding coordinates of $R_{0_j}(H_{\vec{\tau}}(\vec{X}))$. \square

Of course we can build other maps equivariant with respect to the symmetries of the n -cube by taking linear combinations of the maps given by Theorem 2.1. Moreover, calculations similar to those in the preceding proof show that a map $H_{\vec{\tau}}$ is equivariant with respect to the reflections S_j exactly when I is even.

Theorem 2.2. *Let $P : \mathbb{R}^n \rightarrow \mathbb{R}^n$ be a polynomial map with the orientation-preserving symmetries of the n -cube. Then P is a linear combination of maps $H_{\vec{\tau}}$, where $\vec{\tau}$ has tail-uniform parity.*

Proof. Let the k -th coordinate of P have the form

$$\sum_{\vec{i}} a_{k\vec{i}} \vec{X}^{\vec{i}},$$

where $k = 0, \dots, n - 1$. Since P is R_{jk} -equivariant, we have

$$P(R_{jk}^2 \vec{X}) = R_{jk}^2 (P \vec{X}).$$

The j -th coordinate of $P(R_{jk}^2 \vec{X})$ is

$$\sum_{\vec{i}} a_{j\vec{i}} (S_j S_k \vec{X})^{\vec{i}} = \sum_{\vec{i}} (-1)^{\vec{i}_j + \vec{i}_k} a_{j\vec{i}} \vec{X}^{\vec{i}},$$

while that of $R_{jk}^2 (P \vec{X})$ is

$$\sum_{\vec{i}} -a_{j\vec{i}} \vec{X}^{\vec{i}}.$$

Equating like terms, we get $a_{j\vec{i}} = -(-1)^{\vec{i}_j + \vec{i}_k} a_{j\vec{i}}$. Thus, either $a_{j\vec{i}} = 0$ or \vec{i}_j and \vec{i}_k differ in parity. In particular, if $a_{0\vec{i}} \neq 0$ then \vec{i}_0 and \vec{i}_k differ in parity, which implies that \vec{i} has tail-uniform parity.

As an aside, notice that if $a_{0\vec{i}} \neq 0$ and $n > 2$ (so we can pick distinct nonzero indices j and k), the above implies that $a_{j\vec{i}} = 0$ or \vec{i}_j and \vec{i}_k differ in parity. Since the latter possibility has been excluded, it must be that $a_{j\vec{i}} = 0$. Letting other indices play the role of 0 we see that, when $n > 2$, a term that appears in one coordinate cannot appear in any other.

Next we show that, if any term appears, so do terms for every permutation of the exponents. In particular, we claim that if σ is any permutation such that $\sigma(0) = j$ then

$$a_{0\vec{i}} = a_{j\sigma(\vec{i})} (-1)^{I s(\sigma)}.$$

We prove this by induction on the number of transpositions required to write the permutation σ . If $\sigma = 1$ the claim holds, which establishes the base case. We consider two cases, depending on whether the last transposition moves j .

Case 1. Suppose $\sigma = \sigma_{jk} \tau$ where $\tau(0) = k$. By the induction hypothesis,

$$a_{0\vec{i}} = a_{k\tau(\vec{i})} (-1)^{I s(\tau)}.$$

Now R_{jk} -equivariance implies

$$P(R_{jk} \vec{X}) = R_{jk} (P \vec{X}).$$

The j -th coordinate of $P(R_{jk} \vec{X})$ is

$$\begin{aligned} \sum_{\vec{i}} a_{j\vec{i}} (\sigma_{jk} S_k \vec{X})^{\vec{i}} &= \sum_{\vec{i}} a_{j\vec{i}} (S_k \vec{X})^{\sigma_{jk}^{-1} \vec{i}} \\ &= \sum_{\vec{i}} a_{j\sigma_{jk}(\vec{i})} (S_k \vec{X})^{\vec{i}} \\ &= \sum_{\vec{i}} a_{j\sigma_{jk}(\vec{i})} (-1)^{\vec{i}_k} \vec{X}^{\vec{i}}, \end{aligned}$$

while the j -th coordinate of $R_{jk} (P \vec{X})$ is $-a_{k\vec{i}} \vec{X}^{\vec{i}}$. Therefore, $a_{j\sigma_{jk}(\vec{i})} (-1)^{\vec{i}_k} = -a_{k\vec{i}}$ and hence $a_{k\tau(\vec{i})} = -a_{j\sigma_{jk}\tau(\vec{i})} (-1)^{\tau(\vec{i})_k}$. Now $\tau(0) = k$ so $-(-1)^{\tau(\vec{i})_k} = (-1)^I$ and also $s(\sigma) = 1 - s(\tau)$; combining these facts with the induction hypothesis implies $a_{0\vec{i}} = a_{j\sigma(\vec{i})} (-1)^{I s(\sigma)}$, as required.

Case 2. Suppose $\sigma = \sigma_{km} \tau$, where k and m are not j and $\tau(0) = j$. By the induction hypothesis,

$$a_{0\vec{i}} = a_{j\tau(\vec{i})} (-1)^{I s(\tau)}.$$

R_{km} -equivariance implies $P(R_{km} \vec{X}) = R_{km} (P \vec{X})$. The j -th coordinate of $P(R_{km} \vec{X})$ is

$$\begin{aligned} \sum_{\vec{i}} a_{j\vec{i}} (\sigma_{km} S_m \vec{X})^{\vec{i}} &= \sum_{\vec{i}} a_{j\vec{i}} (S_m \vec{X})^{\sigma_{km}^{-1} \vec{i}} \\ &= \sum_{\vec{i}} a_{j\sigma_{km}(\vec{i})} (S_m \vec{X})^{\vec{i}} \\ &= \sum_{\vec{i}} a_{j\sigma_{km}(\vec{i})} (-1)^{\vec{i}_m} \vec{X}^{\vec{i}}, \end{aligned}$$

while the j -th coordinate of $R_{km} (P \vec{X})$ is $a_{j\vec{i}} \vec{X}^{\vec{i}}$. Therefore, $a_{j\sigma_{km}(\vec{i})} (-1)^{\vec{i}_m} = a_{j\vec{i}}$ and hence $a_{j\tau(\vec{i})} = a_{j\sigma_{km}\tau(\vec{i})} (-1)^{\tau(\vec{i})_m}$. Now $\tau(0) = j$ so $(-1)^{\tau(\vec{i})_m} = (-1)^I$ and again $s(\sigma) = s(\tau) + 1$; combining these facts with the induction hypothesis implies $a_{0\vec{i}} = a_{j\sigma(\vec{i})} (-1)^{I s(\sigma)}$ as required.

Now we have established the claim. From the claim we see that for any nonzero term $a_{0,\vec{i}}$ there will be additional nonzero terms for each permutation of \vec{i} . These terms can be taken together to get $a_{0,\vec{i}} H_{\vec{i}}(\vec{X})$. It is also clear from the claim that every nonzero term in any coordinate arises in this

way, hence P is a linear combination of maps of the form $H_{\vec{i}}$, as required. \square

Theorem 2.2 gives a generating set for all the equivariant polynomial maps with the symmetry of the n -cube. This generating set is infinite and contains trivial maps, as seen in our examples. It is known from classical invariant theory that there are finite generating sets for these families over the ring of invariant functions; however, we have found the direct control over exponents in the equivariant polynomials and the uniformity provided by using this infinite generating set is quite effective for constructing examples with the desired symmetries.

3. EXPERIMENTS

The equivariant polynomial maps $H_{\vec{i}}$ of the n -cube have been implemented in the high-level programming language J, which is available both commercially and as freeware. J is described in detail in [Iverson 1995], while [Reiter 1995] gives an introduction targeted to students of mathematical visualization. We give at the bottom of the page the J definition of the map builder, called H. While the code is not easily comprehensible to readers unfamiliar with J, it is offered because of its conciseness and independence on the dimension, and because it provides a compact, complete executable foundation for an exact description of the maps we iterate and use in our experiments.

With that definition of H, we can describe our maps using a notation that is very close to the

mathematical notation we have been using. For example, to define

$$f = H_{(10)} + 0.90H_{(01)} - 0.5H_{(21)} - 0.65H_{(32)}$$

we use the J function `f=: 1 H 1 0 + 0.90 H 0 1 + _0.5 H 2 1 + _0.65 H 3 2`. This is a polynomial map from \mathbb{R}^2 to itself, since the vectors of exponents only have two coordinates. As we have seen, it must have the symmetry of the square. We can see an example of this by iterating f on $(1, 2)$ and $(-2, 1)$, which differ by a 90° rotation. Here are the results of 100, 101, and 102 iterations:

```
f^:(100 101 102) 1 2
_0.6079127 0.371259
_0.3222528 0.864193
0.4268942 0.990321

f^:(100 101 102) _2 1
_0.371259 _0.6079127
_0.864193 _0.3222528
_0.990321 0.4268942
```

One can see that the iterates of the rotation are the same as the rotation of the iterates in this case.

Figure 1, left, shows the result of 25 million iterated images under this map. For each of 100 initial conditions we iterated the map 250,000 times and recorded the images, discarding the first 1000 iterations in each case, so as to remove transient behavior. These runs took place in parallel. Experiments indicate that the attractor is transitive, so this initial point averaging creates the same image that 25 million direct iteration steps would.

```
H=:2 : 0
p=. (i. !#y.)A.i.#y.
s=.x.*_1^(1{y.)*+/@<:@:(#&>)@C."1 p
k=.i.&0"1 p
(+/.*)"1&(k]/.s)@((*/. ^)&(0 1|:k]/.p{y.))
)
```

J-language map builder implementing the creation of equivariant polynomial maps $H_{\vec{i}}$. All elements of the symmetric group \mathfrak{S}_n are encoded by p . The coefficients of the terms are given by s . The “keys” used for organizing the terms into the appropriate coordinates are given by k . Lastly, the resulting map is constructed as the sum of multiples of the coefficients times the appropriate monomials.

(About the color coding: in each figure, pixels visited a low number of times are shown in red, those visited the most are colored magenta, and those in between are given hues ranging from red to magenta around the color wheel. More precisely, for each figure, a frequency table of the frequencies of hits at each pixel is created, logarithms are applied, and a cumulative distribution is created, which is then linearly mapped to the hues. While at times images can be improved by tuning the palette, this scheme seems to be quite effective and is used for Figures 1, 2, and 4.)

The map used for this example uses a perturbation of the parameters produced by a simple random production scheme. In particular, we took linear combinations of four of the H maps where the coefficients were randomly selected from the interval $[-1, 1]$ and the exponents were randomly selected (possibly repeated) tail-uniform vectors with entries less than 4. The resulting map was discarded if its iterates were not finite or if it produced a short cyclic behavior within 20,000 iterations. This was repeated until a map passed that test. Then an image of the iterates was created and the map was discarded unless there were at least five columns of pixels with more than two nonbackground color pixels appearing. The images produced satisfying those requirements were stored for later viewing. A run resulting in 100 such images produced several attractive images.

Figure 1, right, was created in a analogous way, by the iteration of the map

$$-1.756H_{(10)} + 0.256H_{(30)} - 0.6H_{(01)}.$$

This map was also produced in this run of one hundred random examples; however, no perturbation of the parameters was used in this case. Both attractors in Figure 1 have the rotational symmetry of the square, but they are not symmetric with respect to the reflections.

This automatic scheme for generating attractive examples is surely naive, but it seems to be quite successful when applied to dimension two. The

reader may want to refer to [Barany et al. 1993], which describes the use of detectives for determining symmetry. Also, a simple approach to creating attractive images of the iteration of classical complex quadratic maps is described in [Sprott and Pickover 1995].

In dimension three we ran the same scheme, and projected the attractors (with no attempt at hiding pixels behind other pixels) in order to obtain the images to be analyzed. A run of 150 such examples again led to several interesting maps. Figure 2 shows two of them, selected as the most noteworthy because they appear to be low-dimensional (or at least low-volume) attractors and because of the interesting placement of the “hot spots”. The attractor on the left has the reflective symmetries of the cube in addition to the rotational symmetries; the hot spots are associated with faces of a cube. The attractor on the right has only the rotational symmetries, and the hot spots are associated with the edges of a cube. This attractor appears to break up into four loops twirling tightly in three spots each. If these loops were distinct they would form conjugate attractors. However, they coalesce, and experimentally the attractor is transitive, so that the full image is produced upon iterating a single point.

In practice it is easy to perturb the parameters for the map of Figure 2, right, to obtain four conjugate attractors each having C_3 symmetry. It is also possible to perturb the parameters to find three conjugate attractors with C_4 symmetry. Figure 3 shows the results of iterating such a map.

Unlike Figure 2, right, where it is difficult to visualize the quarter-turn rotational symmetries, Figure 3 displays these C_4 symmetries very well. Also notice that the attractor in Figure 3 breaks up into components; it is easy to find perturbations of these parameters that result in connected attractors with C_4 symmetry. We see in this example that although the map is designed to have the rotational symmetries of the cube, the computed attractor may only have the symmetries of a subgroup. In fact, in general some subgroups

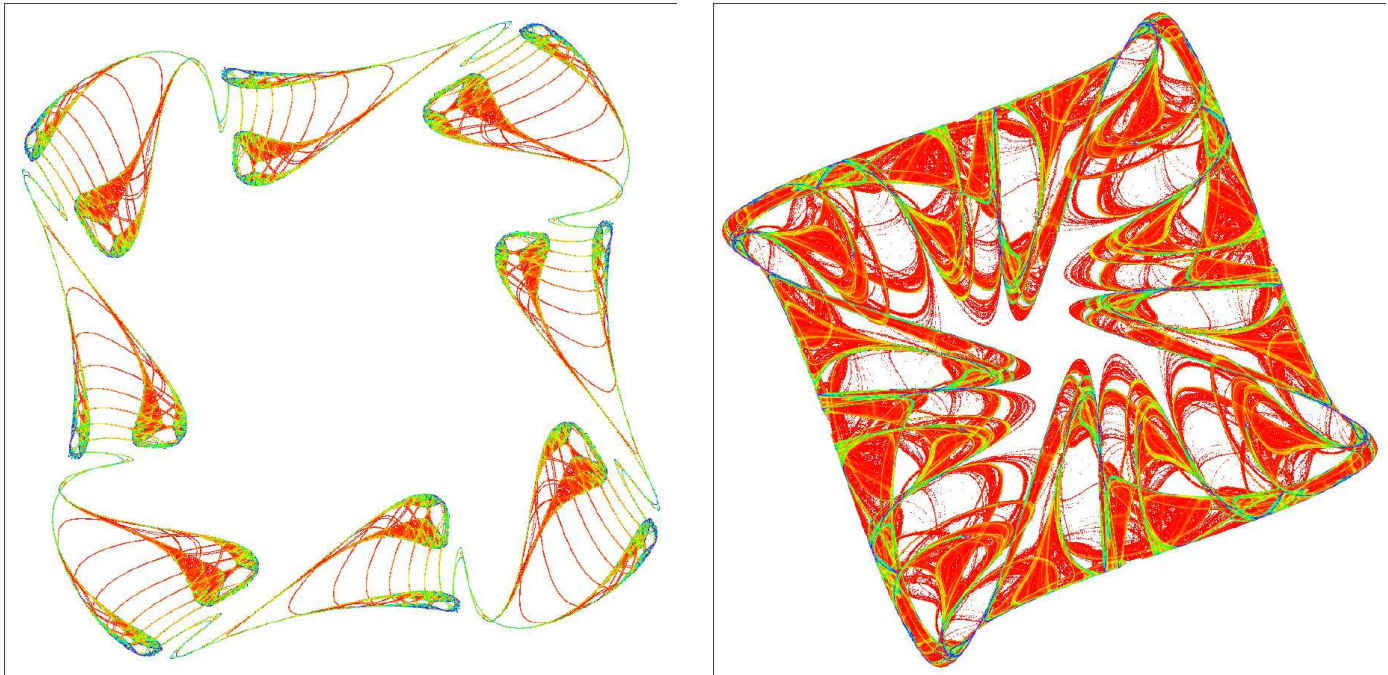


FIGURE 1. Example attractors in two dimensions having the rotational symmetry of the square. On the left is a thin attractor corresponding to the map $H_{\langle 10 \rangle} + 0.90H_{\langle 01 \rangle} - 0.5H_{\langle 21 \rangle} - 0.65H_{\langle 32 \rangle}$. On the right is a thick attractor corresponding to the map $-1.756H_{\langle 10 \rangle} + 0.256H_{\langle 30 \rangle} - 0.6H_{\langle 01 \rangle}$. See top of page 332 for color key.

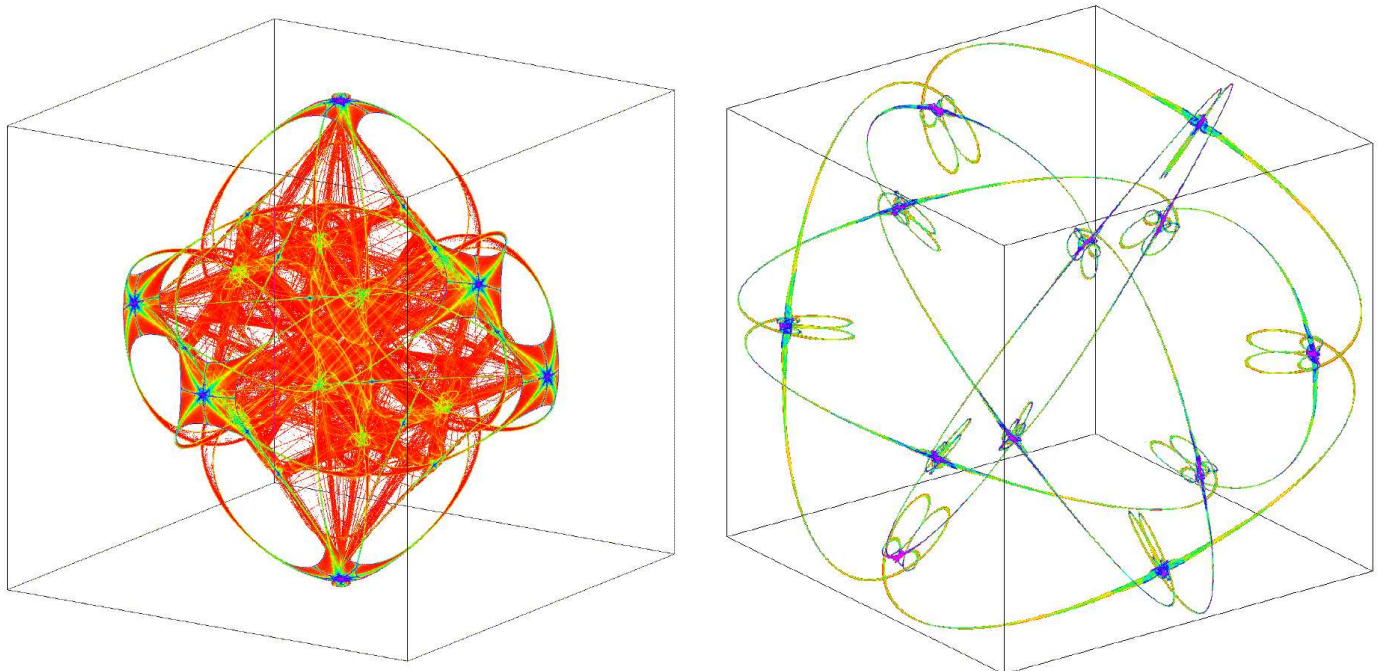


FIGURE 2. Example attractors in three dimensions having the rotational symmetry of the cube. Left: map $-0.882H_{\langle 100 \rangle} + 0.104H_{\langle 300 \rangle} + 0.802H_{\langle 102 \rangle} + 0.792H_{\langle 122 \rangle}$, perpendicular projection from the viewpoint $(2, 3, 1)$; this attractor also has reflective symmetries. Right: map $0.66H_{\langle 100 \rangle} + 0.132H_{\langle 300 \rangle} - 0.962H_{\langle 302 \rangle} + 0.78H_{\langle 031 \rangle}$, perpendicular projection from the viewpoint $(2, 1.5, 1)$.

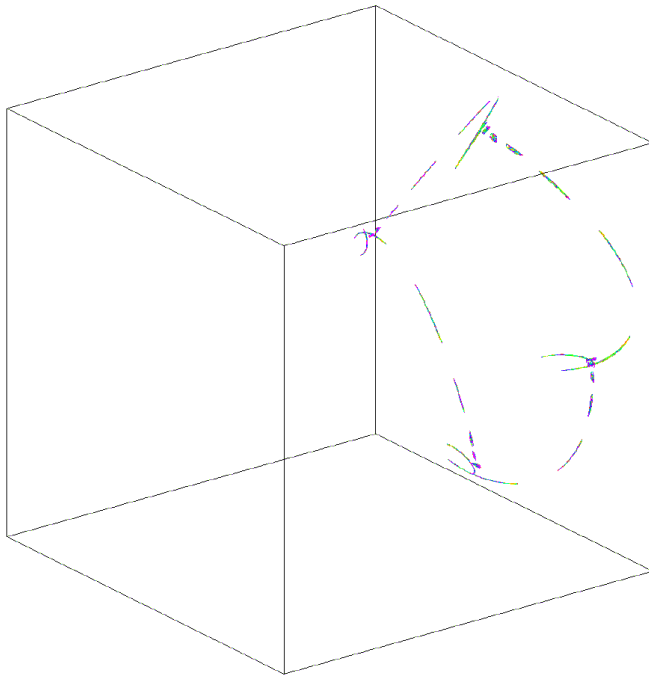


FIGURE 3. Three-dimensional example, with map $0.65H_{\langle 100 \rangle} + 0.132H_{\langle 300 \rangle} - 0.962H_{\langle 302 \rangle} + 0.78H_{\langle 031 \rangle}$.

may not be admissible as the symmetry group of an attractor generated by maps equivariant with respect to a group. The symmetry groups of attractors and restrictions on the subgroups that are admissible are described in [Melbourne et al. 1993; Ashwin and Melbourne 1994]. The necessary background and notation can be found in [Golubitsky et al. 1985], along with a handy subgroup lattice diagram for the group of the rotational symmetries of the cube.

See [Brisson et al. 1996] for several other examples of attractors having the symmetry of the cube.

Attractors in four and higher dimensions can easily be constructed using the same ideas that we used in lower dimensions, but it is far more difficult to achieve a meaningful projection and interesting examples are sparser. In four dimensions we have a good solution to the problem of projecting the attractor in a meaningful way. One of the most symmetric ways of viewing the 4-cube in three-space is to imagine two concentric cubes with corresponding vertices connected. This is often called

the central projection of the 4-cube. We use this projection with a kind of inversion used to fill the interior as follows. We assume for convenience that the points of attractor we are visualizing have been normalized so their coordinates lie between -1 and 1 . Consider the point in 4-space as determined by a point in 3-space, denoted $\vec{v} = \langle x, y, z \rangle$, along with a fourth coordinate, t . When $t = 1$, we want the projection to move the unit cube into the space between the nested cubes with coordinates bounded by ± 2 and ± 3 . If we set

$$\vec{u} = \frac{\vec{v}}{\max(|x|, |y|, |z|)},$$

we can move \vec{v} into the desired space by using $2\vec{u} + \vec{v}$. When $t = -1$, we want the projection to move the unit cube into the space between the nested cubes with coordinates bounded by ± 1 and ± 2 . This time we can move \vec{v} into the desired space by using $2\vec{u} - \vec{v}$. Notice that the minus sign causes a reversal of direction that, along with the translation by $2\vec{u}$, gives a kind of inversion. When t lies between -1 and 1 , we take the corresponding combination, that is, $2\vec{u} + t\vec{v}$. One can also use the Euclidean norm to create the “unit” vector \vec{u} , but we prefer the maximum norm in order to preserve squareness of the edges. Of course, this projection is discontinuous at the origin, but this is not a problem, since we expect a repelling fixed point at the origin.

Figure 4 shows images obtained using this projection. The top part of the figure shows an attractor having hot spots near the 16 vertices of the 4-cube. One can easily see the reflective symmetry between neighboring vertices of the outer cube. The reflection between neighboring vertices of the inner and outer cubes is more difficult to see. The reflection of three perpendicular vectors at a vertex of the outer cube which are facing inward become, under the inversion, three perpendicular vectors at a vertex of the inner cube which are also facing inward; this is to be expected because of one orientation reversal from the reflection and one from the inversion.

The bottom part of the figure shows a relatively thin attractor, with a double diamond shape near each face and “butterflies” in between, where the points of the diamonds get near each other. Since the attractor does not have reflective symmetry, the symmetries are more difficult to observe. This attractor is the only example given here where one might have doubts about long-term stability. The computations usually remained finite for the 500 thousand iterations computed for each of the 400 initial conditions used, but there were occasions when small perturbations of the initial conditions caused numeric overflow. In fact, the image shows examples of “dust” far from the main attractor.

Both attractors in Figure 4 were found by random searches of hundreds of four dimensional examples with higher exponents allowed, and both had parameters tuned. In general, it seems much harder, as one might expect, to randomly discover examples of thin, transitive attractors in higher dimension.

ACKNOWLEDGEMENT

The help of Gabriel Brisson, Kaj Gartz, Benton McCune, and Kevin O’Brien via the work in [Brisson et al. 1996] and the foundation of mathematics and code they developed are greatly appreciated.

REFERENCES

- [Ashwin and Melbourne 1994] P. Ashwin and I. Melbourne, “Symmetry groups of attractors”, *Arch. Rational Mech. Anal.* **126** (1994), 59–78.
- [Barany et al. 1993] E. Barany, M. Dellnitz, and M. Golubitsky, “Detecting the symmetry of attractors”, *Physica D* **67** (1993), 66–87.
- [Brisson et al. 1996] G. Brisson, K. Gartz, B. McCune, K. O’Brien, and C. Reiter, “Symmetric attractors in three-dimensional space”, *Chaos, Solitons and Fractals* **7** (1996), 1033–1051.
- [Cox et al. 1992] D. Cox, J. Little, and D. O’Shea, *Ideals, varieties, and algorithms*, Springer, New York, 1992.
- [Coxeter 1973] H. M. S. Coxeter, *Regular polytopes*, Dover, New York, 1973.
- [Field and Golubitsky 1990] M. Field and M. Golubitsky, “Symmetric chaos”, *Computers in Physics* **4** (1990), 470–479.
- [Field and Golubitsky 1992] M. Field and M. Golubitsky, *Symmetry in chaos*, Oxford U. Press, New York, 1992.
- [Field and Golubitsky 1995] M. Field and M. Golubitsky, “Symmetric chaos: how and why”, *Notices Amer. Math. Soc.* **42** (1995), 240–244.
- [Golubitsky et al. 1985] M. Golubitsky, I. Stewart, and D. Schaeffer, *Singularities and groups in bifurcation theory, 2*, Springer, New York, 1985.
- [Iverson 1995] K. Iverson, *J Introduction and Dictionary*, Iverson Software, Ontario, 1995.
- [Melbourne et al. 1993] I. Melbourne, M. Dellnitz, and M. Golubitsky, “The structure of symmetric attractors”, *Arch. Rational Mech. Anal.* **123** (1993), 75–98.
- [Patera et al. 1978] J. Patera, R. T. Sharp, and P. Winternitz, “Polynomial irreducible tensors for point groups”, *J. Math. Phys.* **19** (1978), 2362–2376.
- [Reiter 1995] C. Reiter, *Fractals, visualization, and J*, Iverson Software, Ontario, 1995.
- [Sprott and Pickover 1995] J. Sprott and C. Pickover, “Automatic generation of general quadratic map basins”, *Computers and Graphics* **19** (1995), 309–313.
- [Stewart and Golubitsky 1992] I. Stewart and M. Golubitsky, *Fearful symmetry*, Blackwell, Cambridge (MA), 1992.
- [Weyl 1952] H. Weyl, *Symmetry*, Princeton U. Press, Princeton, 1952.

Clifford A. Reiter, Department of Mathematics, Lafayette College, Easton, PA 18042 (reiterc@lafayette.edu)

Received November 20, 1995; accepted in revised form July 2, 1996

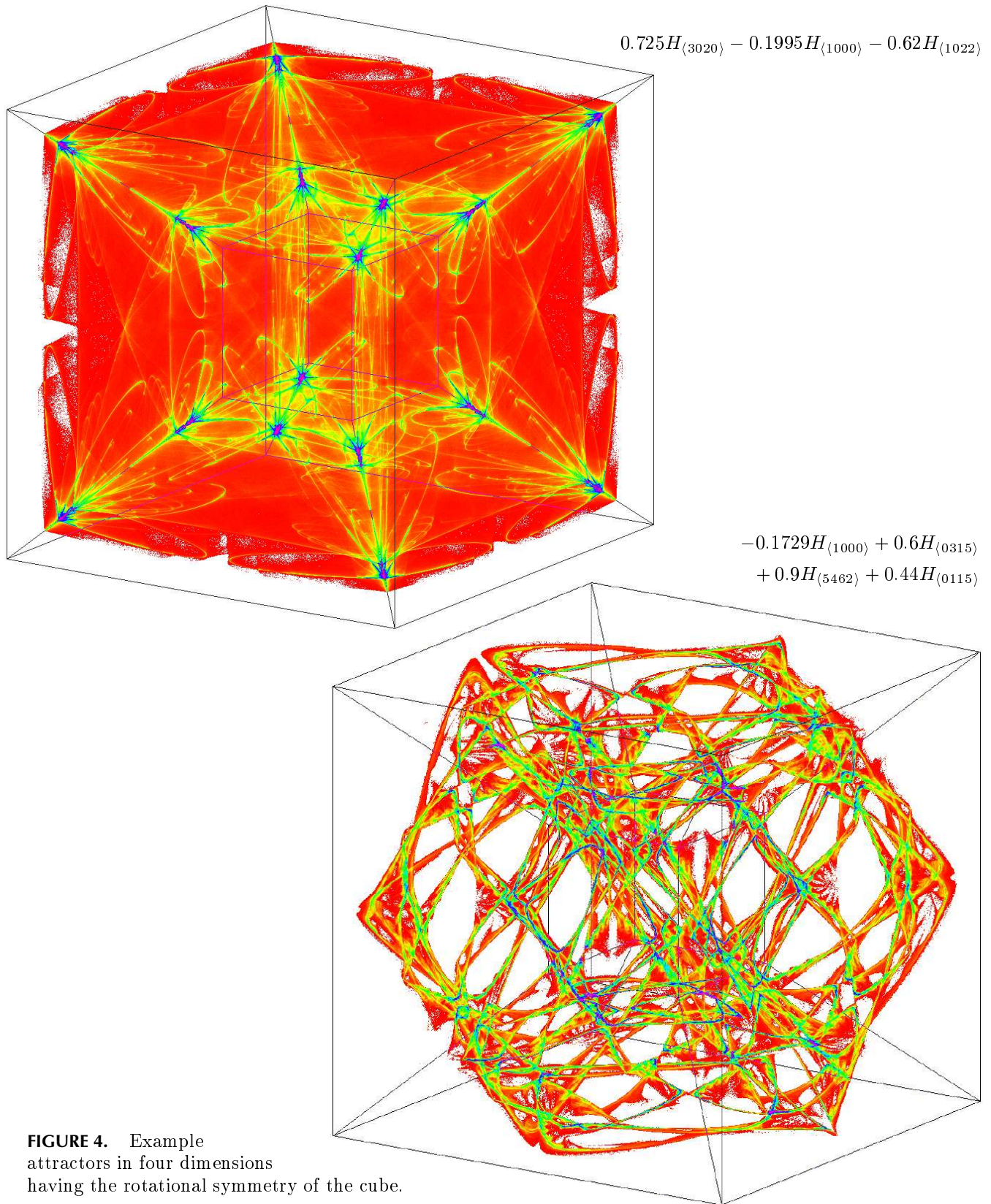


FIGURE 4. Example attractors in four dimensions having the rotational symmetry of the cube.